

# A MATERIAL MODEL FOR TRANSVERSELY ANISOTROPIC CRUSHABLE FOAMS IN LS-DYNA

MAT\_TRANSVERSELY\_ANISOTROPIC\_CRUSHABLE\_FOAM  
MATERIAL LAW 142

**Andreas Hirth**

DaimlerChrysler

HPC X414

71059 Sindelfingen, Germany

Tel.: 07031-90-87781

Fax: 07031-90-87516

email: andreas.hirth@daimlerchrysler.com

**Paul Du Bois**

Consulting engineer

63071 Offenbach/ Main, Germany

**Dr. Klaus Weimar**

DYNAmore

70565 Stuttgart-Vaihingen, Germany

*Keywords:*

Crushable foam, energy absorption, material law, transversely anisotropic

**ABSTRACT**

Recently new materials were introduced to enhance different aspects of automotive safety while minimizing the weight added to the vehicle. Such foams are no longer isotropic but typically show a preferred strong direction due to their manufacturing process. Different stress/ strain curves are obtained from material testing in different directions. A new material model was added to the LS-DYNA code in order to allow a correct numerical simulation of such materials. Ease-of-use was a primary concern in the development of this user-subroutine: we required stress/ strain curves from material testing to be directly usable as input parameters for the numerical model without conversion. The user-subroutine is implemented as MAT\_TRANSVERSELY\_ANISOTROPIC\_CRUSHABLE\_FOAM, Mat law 142 in LS-DYNA Version 960-1106. In this paper we summarize the background of the material law and illustrate some applications in the field of interior head-impact. The obvious advantage of incorporating such detail in the simulation lies in the numerical assessment of impacts that are slightly offset with respect to the foam’s primary strength direction.

**INTRODUCTION**

In this paper we will be studying a class of transversely anisotropic, crushable, low-density foams. Such materials are used in energy-absorbing structures to enhance automotive safety in low velocity (bumper impact, interior head impact) and medium high (pedestrian safety) velocity applications. The potential advantage lies in the high longitudinal strength of the material in comparison to isotropic foams with the same density.

The numerical simulation of such foams requires an anisotropic elastoplastic material law with a flow rule allowing for high permanent volumetric deformation. The anisotropic feature of the material model should thereby allow to properly represent the off-axis material response. In this report existing anisotropic material models for foams in the LS-DYNA code are investigated first. It is shown that they have certain deficiencies rendering them unsuitable to simulate the behavior of anisotropic crushable foams under off-axis loading conditions. Consequently a new material model was developed and added to LS-DYNA as a user-subroutine in order to overcome these problems.

**APPROACH**

*Summary of Test Results*

To quantify the mechanical behavior of anisotropic crushable foams, a testing matrix is proposed containing compression, tension and shear tests according to the following table in figure 1.

loading	Angle $\vartheta$ between load direction and extrusion direction
compression	0°, 5°, 10°, 15°, 25°, 30°, 35°, 45°, 60°, 90°
tension	0°, 90°
shear	0°, 90°

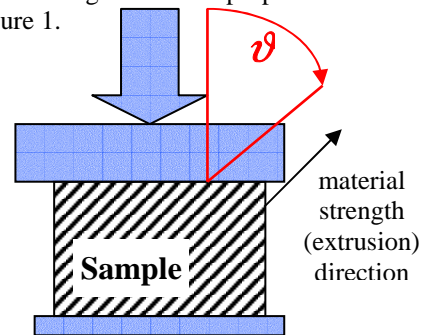


**Figure 1.** Testing matrix and sketch for the compression tests

The samples for offset loading were manufactured by a waterjet cutting technology. At least the compression tests should then be performed quasistatically and dynamically for a number of different strain rates. A typical material with a transversely anisotropic crushable behavior is *Strandfoam*<sup>1</sup>. For this material with a density of 2.5pcf the complete set of tests has been performed.

The rate dependency of these materials will not be treated further here since we want to emphasize the anisotropic aspect of the material behavior. Extension of our material law to include rate dependency is a trivial though extensive matter.

<sup>1</sup> Trademark of the Dow Chemical Company

The main information that can be deduced from the test results is the variation of the foam's compressive strength as a function of the angle  $\vartheta$  between the loading direction and the longitudinal (extrusion- or strong) direction of the foam. The numerical reproduction of the stress/ strain characteristics for the material in different directions is the main issue of this investigation. An example of such a characteristic for *Strandfoam 2.5pcf* is drawn below.

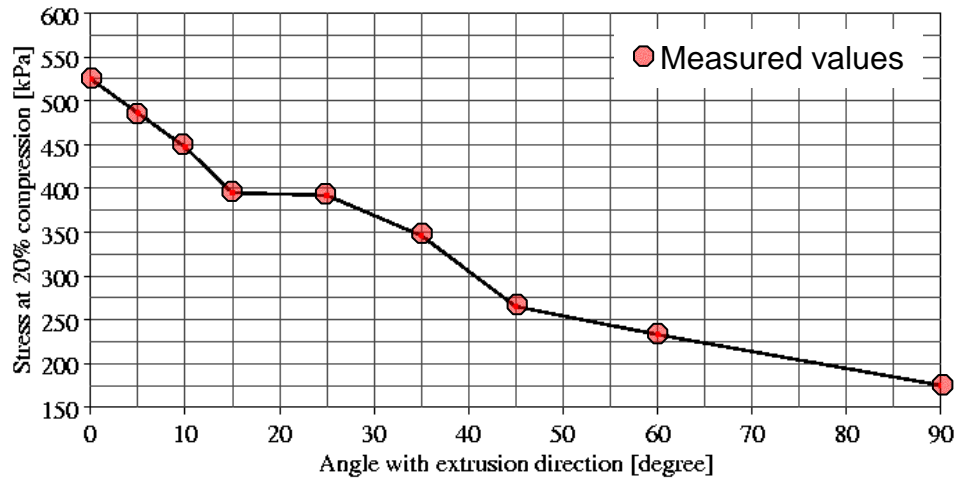


Figure 2. Off-axis strength for *Strandfoam 2.5pcf* at 20% compression

Figure 2 shows the off-axis strength for *Strandfoam 2.5pcf* at 20% compression as taken from the test results (stress values for loading at a strain rate of 10/s). The compressive resistance of the material differs by a factor of 3 between the strong and weak directions and drops fast within the first 15° of oblique loading.

#### Material law *MAT\_HONEYCOMB* (Mat 26)

The only orthotropic, crushable material laws in LS-DYNA suitable for treatment of low density foams (zero Poisson effect) are *MAT\_HONEYCOMB* (Mat 26) and *MAT\_MODIFIED\_HONEYCOMB* (Mat 126). In the *MAT\_HONEYCOMB*, a material reference system is defined by the user. In the case of a transversely anisotropic foam, one of the axes of this system should coincide with the extrusion direction in the undeformed configuration. During the analysis, this material system follows the element rigid body rotation in every brick element. The material law is formulated by uncoupling of the stress tensor components in the material system: every component has a proper yield value independently of the other 5 stress components.

$$|\sigma_{ij}| \leq \sigma_{ij}^y(\epsilon_v) \quad (1)$$

The corresponding yield surface is a rectangular box in principal stress space. This can lead to a surprising behavior of the material model under offset loading. For instance, it is not possible to generate realistic input data for this material law that will lead to an isotropic behavior of the material.

As an example, consider uniaxial loading (in figure 3: compression) in the global x-direction. The material extrusion direction corresponds to the 1-axis of the material system:

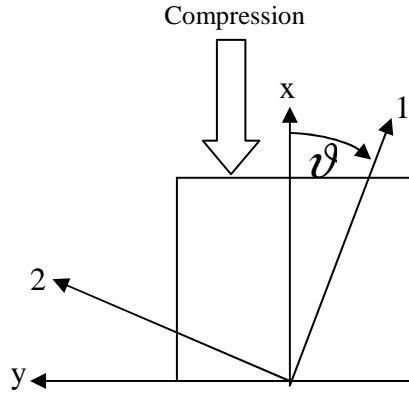


**Figure 3.** Compression of a sample with an extrusion direction at angle  $\vartheta$

If we ignore the third dimension then the stress transformation is:

$$\begin{pmatrix} \sigma_{xx} & 0 \\ 0 & 0 \end{pmatrix} = \begin{pmatrix} \cos\vartheta & \sin\vartheta \\ -\sin\vartheta & \cos\vartheta \end{pmatrix} \begin{pmatrix} -\sigma_{11}^y & -\sigma_{12}^y \\ -\sigma_{12}^y & -\sigma_{22}^y \end{pmatrix} \begin{pmatrix} \cos\vartheta & -\sin\vartheta \\ \sin\vartheta & \cos\vartheta \end{pmatrix} \quad (2)$$

If we assume the deformations to be large enough to cause plastification of all material stress components (other solutions are possible), then (in the case of compression) equation (2) leads to:

$$\begin{pmatrix} \sigma_{xx} & 0 \\ 0 & 0 \end{pmatrix} = \begin{pmatrix} \cos\vartheta & \sin\vartheta \\ -\sin\vartheta & \cos\vartheta \end{pmatrix} \begin{pmatrix} \sigma_{11}^y & \sigma_{12}^y \\ \sigma_{12}^y & \sigma_{22}^y \end{pmatrix} \begin{pmatrix} \cos\vartheta & -\sin\vartheta \\ \sin\vartheta & \cos\vartheta \end{pmatrix} \quad (3)$$

Since all material stress components will be negative and the yield stresses are necessarily positive. Solving equation (3) gives:

$$|\sigma_{xx}| = (\cos\vartheta)^2 \sigma_{11}^y + (\sin\vartheta)^2 \sigma_{22}^y + 2 \cos\vartheta \sin\vartheta \sigma_{12}^y \quad (4)$$

Clearly for known (measured) strong and weak directions in the material, the off-axis strength depends upon the shear strength. The results can be amazing, as for non-zero shear strength, the off-axis strength will exceed the material strength in the principal material axes directions.

Equation (4) was evaluated for angles between 0° and 90° for material data corresponding to *Strandfoam 2.5pcf* and drawn in figure 4 in comparison to the measured values. Off-axis strength is estimated from experimental values for compression at 20% strain, thus using:

$$\begin{aligned} \sigma_{11}^y &= 525 \text{ kPa} & (\vartheta = 0^\circ) \\ \sigma_{22}^y &= 175 \text{ kPa} & (\vartheta = 90^\circ) \\ \sigma_{12}^y &= 175 \text{ kPa} & (\text{shear}) \end{aligned} \quad (5)$$

The predicted overestimation of off-axis strength (figure 4, blue curve) is confirmed in LS-DYNA simulations of compression tests using MAT\_HONEYCOMB (Mat26).

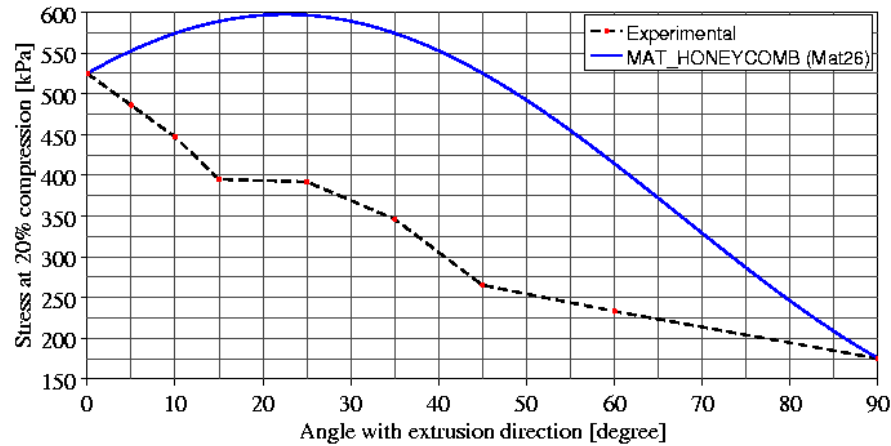


**Figure 4.** Off-axis strength for *Strandfoam 2.5pcf* at 20% compression, experimental values (black dashed line) and theoretical values with Mat26 (blue line)

*Material law MAT\_TRANSVERSELY\_ANISOTROPIC\_CRUSHABLE\_FOAM (Mat 142)*

A user subroutine MAT\_USER\_DEFINED was developed and added at first to LS-DYNA in order to correct the systematic overestimation of the off-axis strength by MAT\_HONEYCOMB (and MAT\_MODIFIED\_HONEYCOMB) for transversely orthotropic material and to allow an easier calibration of the numerical model to measurements. The addition of anisotropic user material laws in LS-DYNA was made possible in a standardized way (/1).

The principal characteristics of the material law in question are the following:

- transversely anisotropic elasto-plastic model
- Tsay-Wu yield surface
- variable coefficients depending upon volumetric strain
- optional definition of a test curve for off-axis loading
- zero Poisson coefficient under longitudinal loads  
(flow surface is spherical in stress space)

A Tsay-Wu surface is a fixed, quadratic surface in 6-dimensional stress-space that is used traditionally as a failure surface for the numerical simulation of composite materials. The application here is quite different since we use the Tsay-Wu surface as a yield surface which is not fixed in stress space, but ‘hardens’ or ‘softens’ as a function of volumetric strain. The evolution of the yield surface is directional and emulates the evolution of the material yield stress along the different material axes.

A further modification of the traditional Tsay-Wu approach lies in the symmetrisation of the yield surface: a single yield value for tension and compression is determined depending upon the current value of the volumetric strain as in equation (6).

$$\varepsilon_v = 1 - \frac{V}{V_0} \Rightarrow \sigma^{yc} = \sigma^{yt} = \sigma^y(\varepsilon_v) \quad (6)$$

Since our applications will mainly consist of a single loading cycle we feel this simplification is justifiable and adds considerably to the numerical robustness of the material model.

With these assumptions the transversely anisotropic Tsay-Wu yield surface is defined as:

$$\begin{aligned}
& F_{11}\sigma_{xx}^2 + F_{22}\sigma_{yy}^2 + F_{22}\sigma_{zz}^2 + \\
& F_{44}\sigma_{xy}^2 + F_{55}\sigma_{yz}^2 + F_{44}\sigma_{zx}^2 + \\
& 2F_{12}\sigma_{xx}\sigma_{yy} + 2F_{23}\sigma_{zz}\sigma_{yy} + 2F_{12}\sigma_{xx}\sigma_{zz} \leq 1
\end{aligned} \tag{7}$$

Thus in equation (7) 6 coefficients have to be determined by matching the following load cases as a function of volumetric strain:

- longitudinal tension and compression ( $F_{11}$ )
- transversal tension and compression ( $F_{22}$ )
- strong shear ( $F_{44}$ )
- weak shear ( $F_{55}$ )
- off-axis tension and compression strong/weak ( $F_{12}$ )
- off-axis tension and compression weak/weak ( $F_{23}$ )

The coefficients of the yield surface are determined for every value of the current volumetric strain from the corresponding yield values of the stress in each material direction.

Under longitudinal compression we obtain equation (8).

$$F_{11} = \frac{1}{\sigma_{xx}^y \sigma_{xx}^y} \tag{8}$$

For the transversal directions we obtain equation (9).

$$F_{22} = \frac{1}{\sigma_{yy}^y \sigma_{yy}^y} \tag{9}$$

Similarly the pure shear condition yields to equation (10) and equation (11).

$$F_{44} = \frac{1}{\sigma_{xy}^y \sigma_{xy}^y} = \frac{1}{\sigma_{zx}^y \sigma_{zx}^y} \tag{10}$$

$$F_{55} = \frac{1}{\sigma_{yz}^y \sigma_{yz}^y} \tag{11}$$

In the classical Tsay-Wu surface, the remaining coefficients are calculated as in equations (12) and (13).

$$F_{12} = \frac{-1}{2} \sqrt{F_{11} F_{22}} \tag{12}$$

$$F_{23} = \frac{-1}{2} F_{22} \tag{13}$$

In our approach it was decided to fit a curve for off-axis loading under theta degrees between longitudinal (=x) and transversal (=y or z) directions in order to determine a reasonable value for  $F_{12}$  as a function of volumetric strain, where  $\sigma_{\theta\theta}$  is the stress, measured in the off-axis loading experiment.

Solving the yield condition under off-axis loading for  $F_{12}$  gives equation (14).

$$F_{12} = \frac{1}{2 \cos^2 \vartheta \sin^2 \vartheta \sigma_{\vartheta\vartheta}^2} - \frac{F_{11} \cos^2 \vartheta}{2 \sin^2 \vartheta} - \frac{F_{22} \sin^2 \vartheta}{2 \cos^2 \vartheta} - \frac{F_{44}}{2} \tag{14}$$

Once all the coefficients of the Tsay-Wu yield function have been determined, it is possible to estimate the off-axis strength of the foam (as we did for material law 26 in figure 4). Again we use the measurements of *Strandfoam 2.5pcf* (see equation (5)) to evaluate an example numerically.

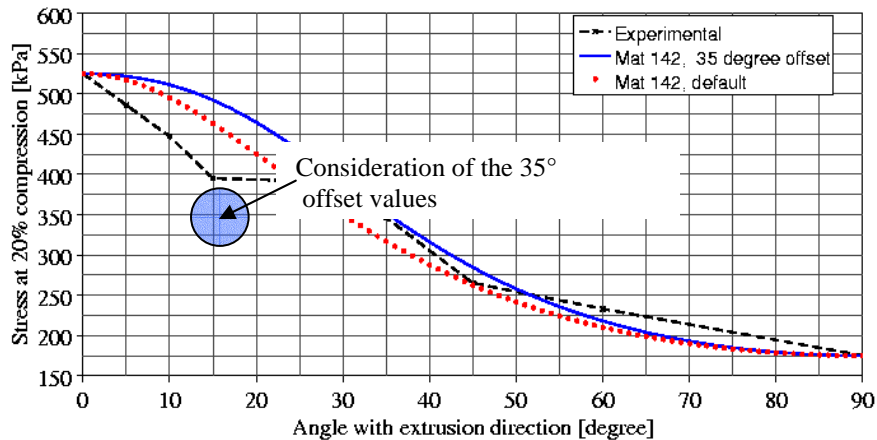


**Figure 5.** Off-axis strength for *Strandfoam 2.5pcf* at 20% compression, experimental values (black dashed line) and theoretical values with Mat 142 (blue line with 35° offset, red dotted line default)

In figure 5 we have compared the values obtained from the default Tsay-Wu model (equation (12), red dotted line) with our modified model where the test curve for loading under 35° was used (equation (14), blue line). In this case it seems, that the default Tsay-Wu gives better overall results than the consideration of the 35° offset values.

#### Validation for Material law *MAT\_TRANSVERSELY\_ANISOTROPIC\_CRUSHABLE\_FOAM (Mat 142)*

A numerical model for *Strandfoam 2.5pcf* was created under the following assumptions :

- Shear stress was compared to transverse stress to show that yield in shear and transverse direction are similar for small strain values, a similar dependency of volumetric strain for shear is assumed in the model as in the transverse direction (i.e. we use the same curve).
- The transition from a plateau-type stress-strain curve to a stress-strain curve with non-zero gradient and generally lower stress values, takes place around 35° offset, therefore the stress-strain curve for loading under 35° was used to construct the yield surface and determine  $F_{12}$ .

Simulations of dynamic compression tests were then performed on a simple model for all tested loading angles at a strain rate of 100/s. The offset loading causes shear deformation as shown in the example in figure 6 (35° offset loading).

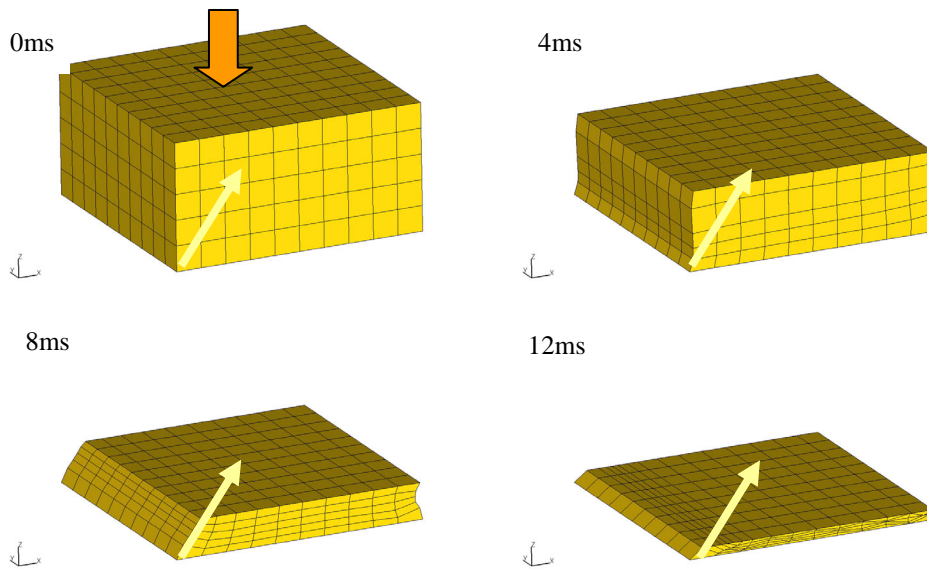


**Figure 6.** Simulation of *Strandfoam 2.5pcf* with 35° offset load (light arrow)

The forces measured under offset loading cannot be directly converted into stress/ strain curves that serve as input for the numerical model. There are a number of reasons for this:

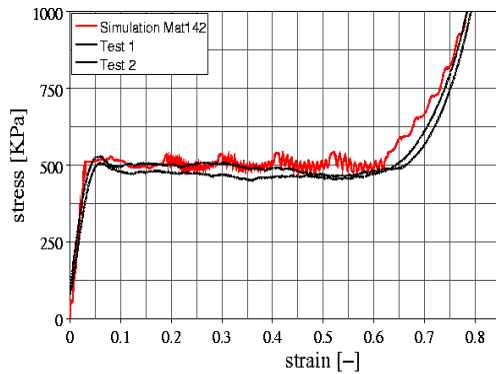
- The shear deformation under off-axis loading means that the angle  $\vartheta$  between loading direction and longitudinal (extrusion) direction of the foam is not constant during the test.
- The friction effects in the test mean that we cannot reproduce the exact boundary conditions, the theoretical derivations in “*Material law MAT\_HONEYCOMB (Mat 26)*” are based on a free sliding boundary condition on both upper and lower surface.
- The state of stress and state of strain are not homogeneous in all samples tested under off-axis loading.

Consequently some trial-and-error might allow a better fit of the model to the measured results.

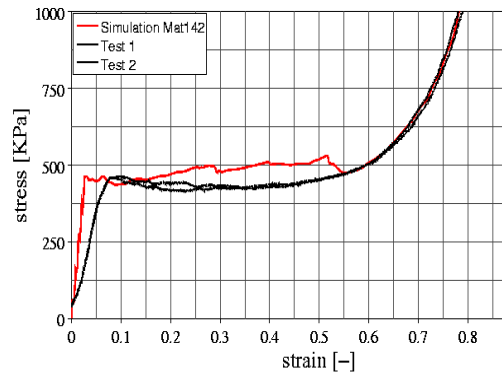
In the following pictures (figure 7) a global overview of simulation and direct comparison to testing is given.



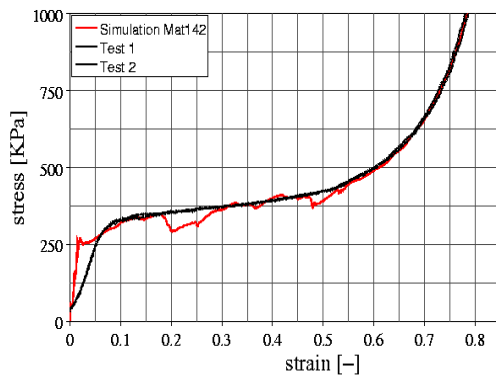
Dynamic compression: 0°



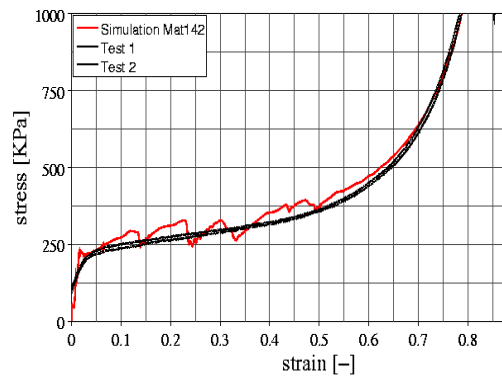
Dynamic compression: 10°



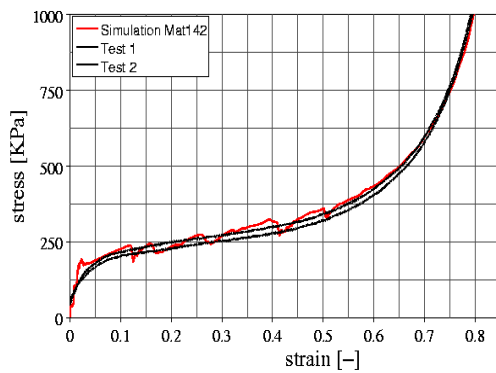
Dynamic compression: 35°



Dynamic compression: 45°



Dynamic compression: 60°



Dynamic compression: 90°

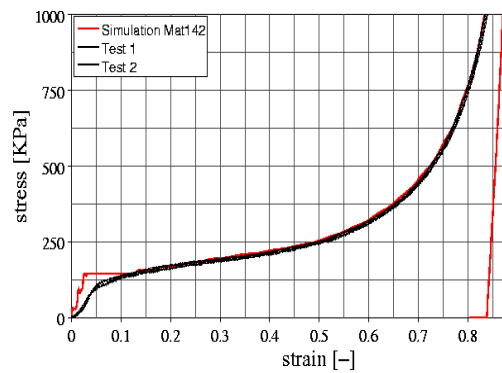


**Figure 7.** Overview of simulation (red line) in comparison to testing (dotted black line)

#### Application to FMVSS201 head-impact

A typical application of the *Strandfoam* material is head-impact protection according to FMVSS201. It is felt that the angle between the impact direction and the extrusion direction of the foam will have an influence on measured headform accelerations. In order to illustrate this, an idealized setup was simulated where the FMVSS201 headform model impacts a rigid inclined plate. The plate is covered with a 15mm thick block of *Strandfoam*, the extrusion

direction of which is varied relative to the normal of the plate ( $0^\circ$ ,  $90^\circ$  and  $-30^\circ$ ). The simulation setup and a typical result are shown in figure 8.

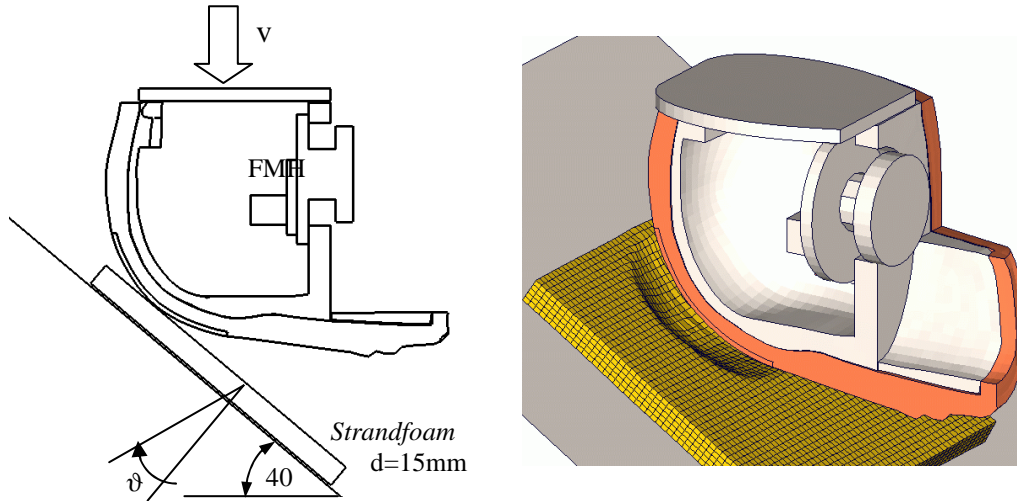


**Figure 8.** left: FMVSS201 headform impacting a skewed plate with *Strandfoam* cover  
right: final deformed shape of the baseline ( $\vartheta = 0^\circ$ )

It should be emphasized that the only modification necessary in the dataset to examine different extrusion directions is the orientation vector in the material law definition. The simulation results in terms of head resultant acceleration time histories are shown in figure 9 for all three different extrusion directions.

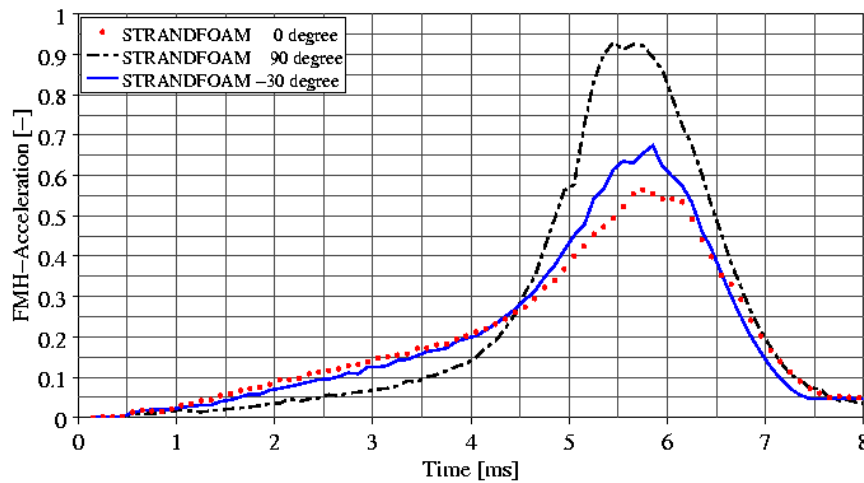


**Figure 9.** Head accelerations with three different extrusion directions in the *Strandfoam*

*Application to honeycomb structures*

One of the main concerns in simulation work for automotive safety today is the modeling of aluminium honeycomb structures that constitute the energy-absorbing component of frontal-offset and side-impact test barriers. To show the potential of the newly developed material model in this field we have simulated an impact test of the *Cellbond honeycomb* barrier against a concrete pole. The simulation was first performed using material law 26 in LS-DYNA and repeated while switching the material model to law 142. The final deformed shapes for both simulations are shown below in figure 10.

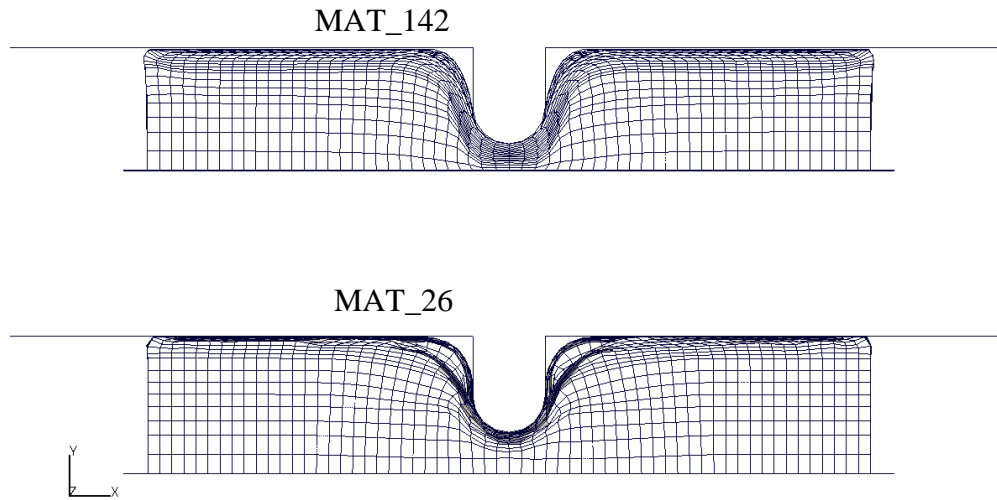


**Figure 10.** Final deformed shape of simulation using material laws 142 and 26

Although both input decks use the same stress-strain functions describing the honeycomb response in its strong and weak directions, the resulting strength under offset loading is a function of the material formulation as shown in figure 11. Here the off-axis strengths were determined as described in paragraph “*Material law MAT\_HONEYCOMB (Mat 26)*”.

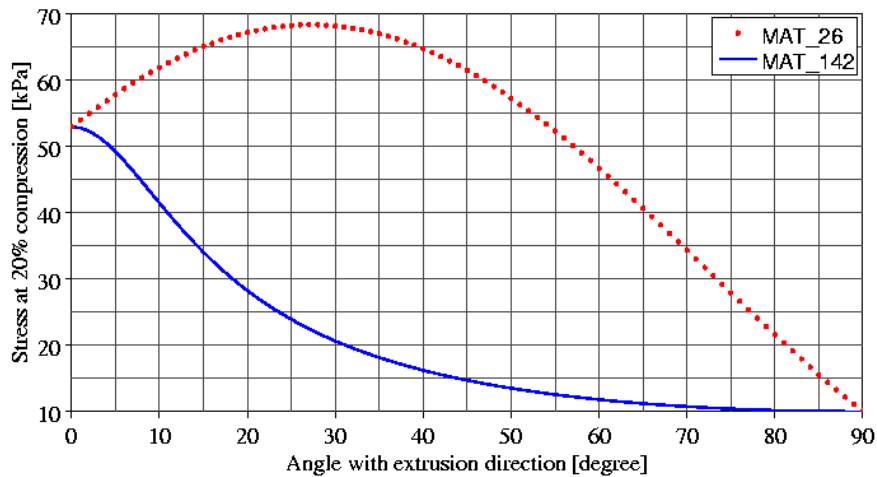


**Figure 11.** Off-axis strength for *Cellbond honeycomb* at 20% compression, theoretical values with Mat26 (red dotted line) and Mat142 (blue line)

The impact forces as a function of time resulting for both simulations are shown and compared to test values in figure 12. As could be expected, the simulation based on material law 26 shows a too high energy absorption prior to 60 milliseconds, and consequently no densification occurs in this model.

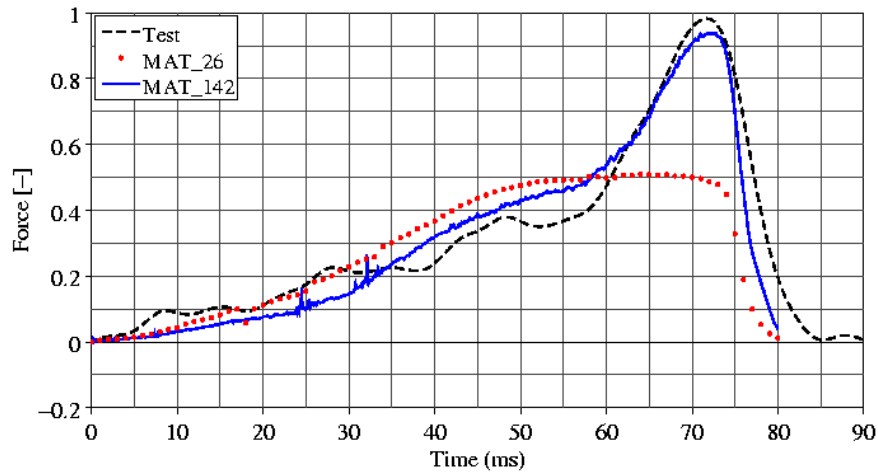


**Figure 12.** Overview of simulation using material law 26 (dotted red line) and material law 142 (blue line) in comparison to testing (dashed black line)

### SUMMARY OF CONCLUSIONS

A transversely anisotropic crushable material model for low-density foams was developed. The results in the simulation of *Strandfoam* allow the numerical simulation of the off-axis material response with good accuracy. Another possible application lies in the simulation of honeycomb for barriers used in frontal-offset and side-impact testing.

### REFERENCES

1. LS-DYNA, structured user's manual, version 950, LSTC